

Detection of Lyman- α emitting galaxies at redshift $z = 4.55$

Esther M. Hu^{*,†}

and

Richard G. McMahon[‡]

To appear in Nature

arXiv:astro-ph/9606135v1 21 Jun 1996

*Institute for Astronomy, University of Hawaii, 2680 Woodlawn Drive, Honolulu, Hawaii 96822, USA

†Visiting Astronomer, W. M. Keck Observatory, California Association for Research in Astronomy.

‡Institute of Astronomy, University of Cambridge, Madingley Road, Cambridge CB3 0HA, UK

Studies of the formation and early history of galaxies have been hampered by the difficulties inherent in detecting faint galaxy populations at high redshift. As a consequence, observations at the highest redshifts ($3.5 < z < 5$) have been restricted to objects that are intrinsically bright. These include quasars, radio galaxies, and some Ly α -emitting objects^{1–3} that are very close to (within ~ 10 kpc) — and appear to be physically associated with — quasars. But the extremely energetic processes which make these objects easy to detect also make them unrepresentative of normal (field) galaxies. Here we report the discovery of two Ly α -emitting galaxies at redshift $z = 4.55$, which are sufficiently far from the nearest quasar (~ 700 kpc) that radiation from the quasar is unlikely to provide the excitation source of the Ly α emission. Instead, these galaxies appear to be undergoing their first burst of star formation, at a time when the Universe was less than one billion years old.

Searches for high- z field galaxies have progressed from several directions. Extensive spectroscopic surveys of field galaxies^{4–7} now show numerous random field galaxies at $z > 1$, with evidence that many of these are in the process of intense star formation.⁸ Searches for the galaxies associated with quasar absorption lines are also beginning to turn up normal galaxies in this redshift range.⁹ At $z > 1.7$, where the [O II] emission line at 3,727 Å is no longer detectable in the optical window, we are beginning to find objects on the basis of their UV absorption lines.^{10–13} These objects may be starbursting galaxies, in some cases with active galaxy (AGN) activity.

At redshifts near 3, absorption-line objects should also show distinct continuum color breaks as the limit for the hydrogen Lyman series (912 Å in the rest frame) becomes observable at ultraviolet wavelenths. The objects identified by color breaks and UV absorption features to lie at $3.0 < z < 3.5$ [ref. 13] should be relatively evolved galaxies, whose bright UV continua are produced by massive stars which chemically enrich these systems, giving rise to metal-line absorption features and dust, making Ly α emission weak or undetectable.

Galaxies at earlier stages of this process, prior to the formation of dust, may have much stronger Ly α emission relative to the stellar continuum. Such objects, which are faint in the continuum, may be hard to pick out with color break techniques but relatively easy to find by Ly α searches. A small number of such objects have been seen in the fields of $z \sim 2 \rightarrow 3.5$ quasars, which are well separated from the quasar and which may represent neighboring galaxies either with AGN¹⁴ or with intense star formation that can excite the Ly α emission line but without so much dust that the line is suppressed.^{15–17} The latter class of objects, which are relatively unobscured by foreground absorption, may provide the most direct estimates of star formation at the earliest epochs. It appears that the quasar

may mark the sites of such formation and thus identify a redshift for targeted wavelength searches.¹⁸ The present paper reports detection of such objects at by far the highest redshift yet in the field of the $z = 4.55$ quasar BR2237–0607.¹⁹

In order to search for high- z objects in the fields of the $z > 4$ quasars, we first obtained exposures through a narrow-band filter centered on the quasar’s redshifted Ly α emission, and through a nearby broader continuum, with a Tektronix 2048² camera on the Univ. of Hawaii’s 2.2-m telescope. Five $z > 4$ quasar fields have now been imaged, but the spectroscopic follow-up is complete only for BR2237–0607, which we describe here. Narrow-band and continuum images on this field are shown in Fig. 1. All objects with a significant excess in the Ly α bandpass were considered candidate Ly α emitters, and this initial search turned up 10 objects in the 19.25’ field surrounding BR2237–0607, a subsample of which is circled in Fig. 1. However, many of these candidate objects correspond to lower redshift galaxies whose emission lines coincidentally match the redshifted Ly α wavelength, or to objects whose continuum shape makes them significantly brighter in the narrow-band filter. Therefore, in order to proceed further we obtained simultaneous spectra of the candidate objects using the multi-object LRIS spectrograph²⁰ on the Keck 10-m. telescope.

Two-dimensional spectra for the three candidate objects of Fig. 1 are shown in Fig. 2, with the wavelength region of the narrow-band and reference continuum band filters marked at the top of the plot. As expected, most of the candidate objects were identified as $z < 1$ galaxies. We show in this figure, for instance, the spectrum of the low-redshift emission-line galaxy, LA10, where the strong emission is identified with the [O II] 3,727 Å line instead of Ly α , for a redshift of 0.802. The spectra show various features that are hallmarks of this class of interloper, namely: much stronger continuum, including clearly detected flux from the region below 5,000 Å which would correspond to the Lyman limit break at the rest-frame 912 Å photoionization threshold of neutral hydrogen for $z \sim 4.6$ objects; and the offset wavelength position near the edge of the narrow passband filter. However, the two objects denoted here as LA1 and LA2 exhibit only an extremely strong single emission line close to the central wavelength of the narrow-band filter together with an extremely weak continuum. The insets for Fig. 1 show that for LA1 the continuum is undetected even in an extremely deep 1-hour I -band image obtained with LRIS on Keck, while a weak diffuse structure is seen in this band for LA2, whose continuum is also faintly detected in the spectroscopic data. The Kron-Cousins I magnitude of LA2 is 24.69 and it is detected at the 4σ level in the Keck I -band image (Table 1). Spectra of these two objects are shown in Fig. 3. A useful measure of the relative strength of line to continuum is the equivalent width, which is defined as the width of a rectangle with the same area as an emission (or absorption) feature, with a height equal to the continuum level above zero. The observed equivalent widths (> 700 Å [LA2] and $> 1,300$ Å [LA1]) are quoted only as lower limits because of the weakness of

the continuum, but are too large for these lines to be [O II] or H α ^{21–23} — an interpretation which is also ruled out by the absence of any other strong emission lines. This leaves little alternative but to identify these objects as Ly α emitters at the redshift of the quasar. Their coordinates and properties may be found in Table 1. The equivalent width of object LA10 (123 Å) is consistent with the expected range of values for [O II] emission.^{4,7}

The separations from the quasar of 117'' for LA1 and 105'' for LA2 are too large for the quasar to have a significant role in exciting the objects²⁴ (1'' = 7.1 h^{-1} kpc at $z = 4.55$, where $h = H_0/100$ km s⁻¹ Mpc⁻¹ and $q_0=0.5$) and it appears that the objects must be either internally excited or ionized by the general metagalactic UV flux.²³ As can be seen from the inset to Fig. 1, LA1 is quite compact and could have an AGN component, although there is no sign of emission from C IV at 1,549 Å. However, LA2 is quite diffuse in both I and Ly α , and most likely is excited by star formation. An alternative possibility is that the Ly α emission is produced by surface ionization of the gas cloud by the metagalactic UV flux. The metagalactic ionizing flux at these wavelengths is currently estimated²⁵ as $1 - 3 \times 10^{-22}$ erg cm⁻² s⁻¹ Hz⁻¹ sr⁻¹, which would produce an observed Ly α flux of $\sim 2 \times 10^{-17}$ erg cm⁻² s⁻¹ from an object with a 2'' angular size at $z = 4.55$ (ref. 23) if there is one Ly α photon emitted per ionization and we see only the forward side of the cloud, so it is possible we are seeing a component due to ionized gas clouds. However, this would provide no explanation for the continuum light in LA2.

The rest frame equivalent widths of the systems are around > 130 Å (LA2) and > 240 Å (LA1), which are marginally consistent with stellar excitation for an initial mass function dominated by massive stars.²⁶ Following the discussion of the previous paragraph, the Ly α may arise from a combination of internal and external ionization. If the observed emission were primarily due to stars, and there were no internal scattering and extinction, then the luminosity of 3×10^{42} h^{-2} erg cm⁻² s⁻¹ ($q_0=0.5$) would correspond to a star formation rate in solar masses (M_\odot) per year of ~ 3 h^{-2} M_\odot yr⁻¹, where we use Kennicutt's (ref. 21) relation between H α luminosity and star formation rate (SFR) of $\text{SFR} = L(\text{H}\alpha) \times 8.9 \times 10^{-42}$ erg s⁻¹ M_\odot yr⁻¹, and assume a ratio of Ly α to H α (8.7) that applies for Case B recombination.²⁷ Given the Hubble time at this redshift of 7×10^8 h^{-1} yr ($q_0=0.5$) the integrated amount of star formation is small compared to that of a 'normal' galaxy with 6×10^{10} h^{-1} M_\odot of stars (a so-called L^* galaxy).

Because of the targeted nature of the search it is hard to estimate from the present data whether such objects may be common in the general field or whether they are preferentially found around quasars. Observations, currently in progress, of additional quasars and blank field regions should answer this question.

REFERENCES

1. Hu, E. M., McMahon, R. G. & Egami, E. *Astrophys. J.* **459**, L53–L57 (1996). [astro-ph/9512165]
2. Fontana, A., Cristiani, S., D’Odorico, S., Giallongo, E. & Savaglio, S. *Mon. Not. R. astr. Soc.* **279**, L27–L30 (1996). [astro-ph/9601086]
3. Petitjean, P., Pécontal, E., Valls-Gabaud, D. & Charlot, S. *Nature* **380**, 411–413 (1996). [astro-ph/9603088]
4. Songaila, A., Cowie, L. L., Hu, E. M. & Gardner, J. P. *Astrophys. J. Suppl.* **94**, 461–515 (1994).
5. Lilly, S. J., LeFèvre, O., Crampton, D., Hammer, F. & Tresse, L. *Astrophys. J.* **455**, 50–59 (1995). [astro-ph/9507010]
6. Glazebrook, K., Ellis, R., Colless, M., Broadhurst, T., Allington-Smith, J., & Tanvir, N. *Mon. Not. R. astr. Soc.* **273**, 157–168 (1995). [astro-ph/9503116]
7. Cowie, L. L., Songaila, A., Hu, E. M. & Cohen, J. G. *Astr. J.* (in the press). [astro-ph/9606079]
8. Cowie, L. L., Hu, E. M. & Songaila, A. *Nature* **377**, 603–605 (1995). [astro-ph/9510045]
9. Dickinson, M. & Steidel, C. *Bull. Amer. Astr. Soc.* **27**, 849 (1995).
10. Cowie, L. L., Songaila, A., Hu, E. M., Egami, E., Huang, J.-S., Pickles, A. J., Ridgway, S. E., Wainscoat, R. J., & Weymann, R. J. *Astrophys. J.* **432**, L83–L86 (1994).
11. Egami, E., Iwamuro, F., Maihara, T., Oya, S. & Cowie, L. L. *Astr. J.* (in the press). [astro-ph/9604135]
12. Yee, H. K. C., Ellingson, E., Bechtold, J., Carlberg, R. G. & Cuillandre, J.-C. *Astr. J.* **111**, 1783–1794 (1996). [astro-ph/9602121]
13. Steidel, C. C., Giavalisco, M., Pettini, M., Dickinson, M. & Adelberger, K. L. *Astrophys. J.* **462**, L17–L21 (1996). [astro-ph/9602024]
14. Lowenthal, J. D., Hogan, C. J., Green, R. F., Caulet, A., Woodgate, B. E., Brown, L., & Foltz, C. B. *Astrophys. J.* **377**, L73–L77 (1991).
15. Giavalisco, M., Macchetto, F. D. & Sparks, W. B. *Astr. Astrophys.* **288**, 103–121 (1994).

16. Macchetto, F. D., Lipari, S., Giavalisco, M., Turnshek, D. A. & Sparks, W. B. *Astrophys. J.* **404**, 511–520 (1993).
17. Francis, P. J., Woodgate, B. E., Warren, S. J., Møller, P., Mazzolini, M., Bunker, A. J., Lowenthal, J. D., Williams, T. B., Minezaki, T., Kobayashi, Y., & Yoshii, Y. *Astrophys. J.* **457**, 490–499 (1996). [astro-ph/9511040]
18. Djorgovski, S., Spinrad, H., McCarthy, P. & Strauss, M. *Astrophys. J.* **299**, L1–L5 (1985).
19. Storrie-Lombardi, L. J., McMahon, R. G., Irwin, M. J. & Hazard, C. *Astrophys. J. Suppl.* (in the press). [astro-ph/9604021]
20. Oke, J. B., Cohen, J. G., Carr, M., Cromer, J., Dingizian, A., Harris, F. H., Labrecque, S., Lucinio, R., Schaal, W., Epps, H., & Miller, J. *Publ. astr. Soc. Pacif.* **107**, 375–385 (1995).
21. Kennicutt, Jr., R. C. *Astrophys. J.* **272**, 54–67 (1983).
22. Kennicutt, Jr., R. C. *Astrophys. J.* **388**, 310–327 (1992).
23. Songaila, A., Cowie, L. L. & Lilly, S. J. *Astrophys. J.* **348**, 371–377 (1990).
24. Hu, E. M., Songaila, A., Cowie, L. L. & Stockton, A. *Astrophys. J.* **368**, 28–39 (1991).
25. Williger, G. M., Baldino, J. A., Carswell, R. F., Cooke, A. J., Hazard, C., Irwin, M. J., McMahon, R. G., & Storrie-Lombardi, L. J. *Astrophys. J.* **428**, 574–590 (1994).
26. Charlot, S. & Fall, S. M. *Astrophys. J.* **415**, 580–588 (1993).
27. Brocklehurst, M. *Mon. Not. R. astr. Soc.* **153**, 471–490 (1971).
28. Massey, P., Strobel, K., Barnes, J. V. & Anderson, E. *Astrophys. J.* **328**, 315–333 (1988).
29. Stone, R. P. S. *Astrophys. J.* **218**, 767–769 (1977).
30. Landolt, A. U. *Astr. J.* **104**, 340–371 (1992).

Acknowledgements

We thank T. Bida, R. Campbell, T. Chelminiak, and B. Schaefer for their assistance in obtaining the observations, which would not have been possible without the LRIS spectrograph of J. Cohen and B. Oke. Research at the University of Hawaii was supported by the

State of Hawaii and by NASA. E.M.H. would also like to gratefully acknowledge a University Research Council Seed Money grant. R.G.M. acknowledges the support of the Royal Society.

Fig. 1.— Central $3'.5 \times 3'.5$ region showing the $z = 4.55$ quasar BR2237–0607 and emitting objects LA1, LA2, and LA10 in a narrow-band filter (central wavelength 6,741 Å, 51 Å bandpass) centered on the quasar’s redshifted Ly α emission [left panel] and through a nearby broad, line-free continuum filter (7,500 Å, 698 Å bandpass) [right panel]. Inset panels show the region around identified Ly α emitters LA1 and LA2, both in line and continuum, and enlarged by a factor of two. Here the continuum is a deep 1 hr *I* band taken at Keck. LA2 has a weak continuum (Fig. 2), but is clearly extended in both the Ly α and *I*-band images. The continuum for LA1 is not detected in the 1-hr *I*-band exposure at a 1σ magnitude of 26.15. The data were taken as a series of sky noise-limited integrations, with an offset step of $10''$ between successive frames, and a median sky exposure was generated from the on-field exposures for each night and used to correct for non-uniformities in detector response (flat-field). Spectrophotometric standards (Feige 15, Feige 110, Kopff 27, BD+28 4211)^{28,29} for the narrow-band data and a combination of spectrophotometric (Feige 110, BD+28 4211)²⁹ and Landolt standards (in the fields of SA 92-248, PG1633+099, PG0231+051)³⁰ for the continuum data were used to calibrate the data, and were taken in observations both before and after the target exposures. The composite image quality was $1''.0$ in both the 20.8 hr narrow-band image and in the 1 hr 7,500 Å continuum image, and $0''.8$ in the deep 1 hr Keck *I*-band image.

Fig. 2.— LRIS spectra of the 3 candidates from Fig. 1 in the BR2237–0607 field. Observations were made with a multi-slit mask over the quasar field, with a slit width of $1''.4$, spectral resolution of ~ 17 Å, and spatial sampling of $0''.215/\text{pixel}$. The results of 3 hrs exposure in a single mask setting are shown as two-dimensional spectra, with night sky lines subtracted from the spectrum, and the displaced starting wavelengths reflect the offsets in slit position for different objects in the field. The spatial extent of each spectrum is $\sim 6''.5$ — roughly the diameter encircling the objects in Fig. 1. At the top of the plot we indicate the wavelength regions covered by the narrow-band filter (central wavelength 6,741 Å, 51 Å bandpass), which is centered near the wavelength of the quasar’s Ly α emission, and the reference continuum filter (central wavelength 7,500 Å, 698 Å bandpass). Objects LA1 and LA2, which are well centered in the narrow-band filter, have observed equivalent widths in excess of 700 Å in the emission line, and thus must almost certainly be due to redshifted Ly α . No other features are detected, apart from a faint continuum in LA2. Object LA10 is an [O II] emitter at $z = 0.802$ with a line equivalent width of ~ 123 Å, and can be easily identified, even in the absence of other emission lines, by its strong continuum, extending blueward of 5,000 Å (roughly, the wavelength of the break in the Lyman limit absorption for $z \sim 4.6$ objects). The asymmetric placement of the emission line is another clue of a low- z interloper.

Fig. 3.— Extracted spectra for LA1 and LA2 plotted in the rest wavelength frame. The spectra represent a total of 4.7 hrs integration with the LRIS spectrograph on Keck. The emission wavelengths agree to within $\sim 2.4 \text{ \AA}$ ($\sim 100 \text{ km s}^{-1}$ at $z = 4.55$; $\sim 0.4 \text{ \AA}$ in the rest frame) for these two objects. LA1 is not resolved at 3.1 \AA in the rest frame, and the width of LA2 is most likely due to the extended emission structure across the slit.

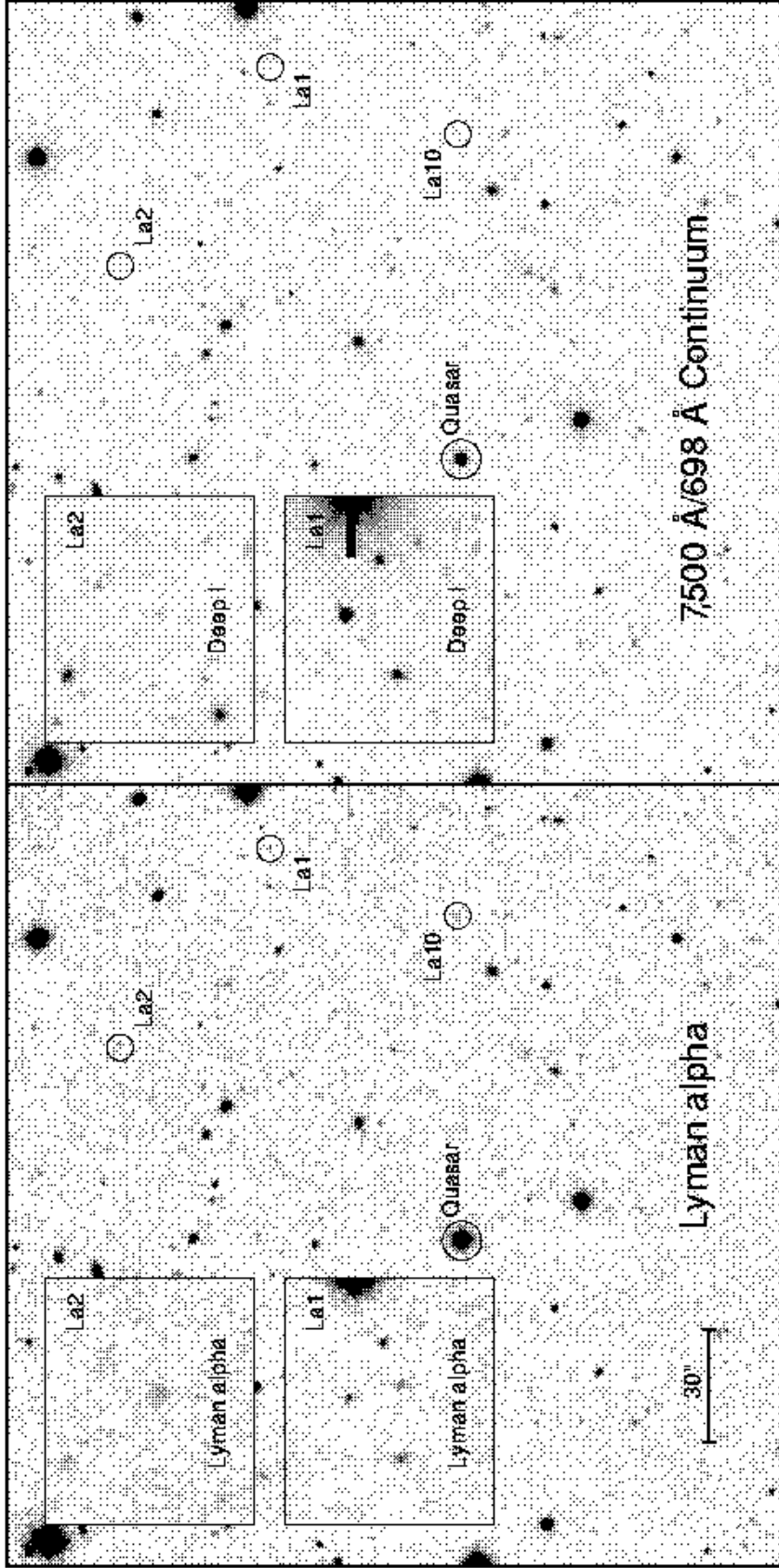


Fig. 1.

Redshift 4.55 Lyman alpha Candidates in BR2237-0607 Field

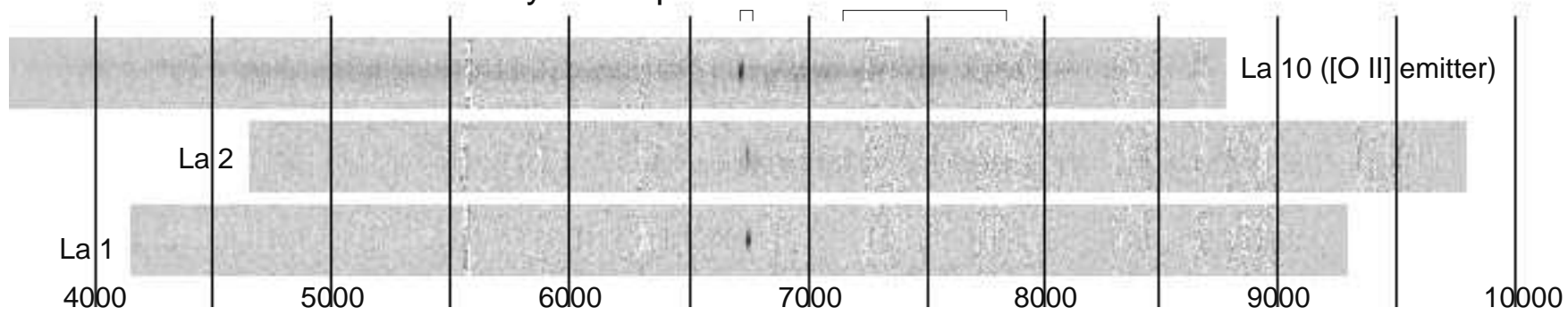


Fig. 2.—

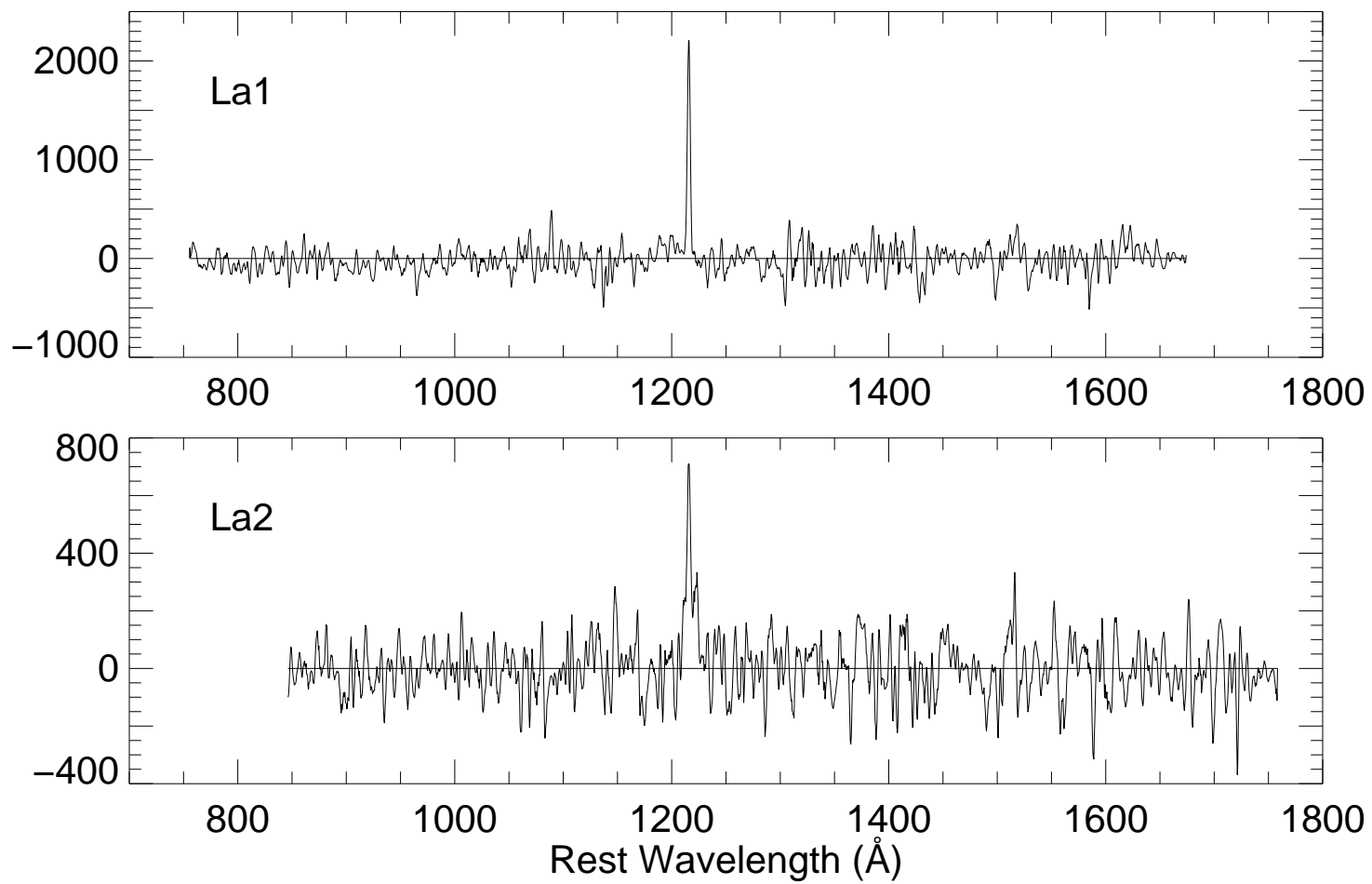


Fig. 3.—

TABLE 1. BR2237–0607 Candidate Identifications

Object	z	R.A. (1950)	Dec. (1950)	Flux (6741Å) (ergs cm ² s ⁻¹)	m_{6741}	m_{7500}	m_I
QSO	4.558 [†]	22 ^h 37 ^m 17 ^s .40	−06° 07′ 59″.7	2.4×10^{-14}	16.57	17.99	...
LA1	4.551	22 ^h 37 ^m 10 ^s .35	−06° 07′ 08″.6	5.0×10^{-17}	23.60	> 24.89	> 26.15
LA2	4.550	22 ^h 37 ^m 13 ^s .92	−06° 06′ 28″.2	6.7×10^{-17}	23.06	24.81	24.69
			$\langle 1\sigma \rangle$	1.5×10^{-17}	24.92	24.89	26.15

Notes to Table 1.

Object coordinates were determined by applying astrometric fits for plate scale and rotation, and fitting to the Cambridge Automatic Plate Measuring (APM) Survey object positions in the quasar field and in calibration star fields taken before and after the quasar observations. We estimate the relative position accuracy of these coordinates to have typical errors less than 0″.2 – 0″.3. Magnitudes, fluxes, and their 1 σ errors are measured over 3″ diameter apertures. The narrow-band and adjacent continuum-band filter measurements (m_{6741} and m_{7500}) are given as equivalent visual (AB) magnitudes, for ease of conversion to emission-line fluxes, which are quoted with continuum contributions subtracted. Keck I -band magnitudes are on the Kron-Cousins system, and were tied to I -band photometry on this field using the UH 2.2-m telescope (Keck I zero point = 27.46). The quasar is saturated on the deep Keck I -band image.

[†]From Storrie-Lombardi’s estimate (ref. 19) based on O I 1304 Å, Si/O IV 1400 Å, and C IV 1549 Å. Simultaneous observations of the quasar were not possible without dropping one or more of the potential candidates from the mask.